



SUPPLEMENTARY MATERIAL TO
Different electrode modification protocols for evaluating the water-splitting properties of a P(V)-metalloporphyrin

BOGDAN-OVIDIU TARANU*

National Institute of Research and Development for Electrochemistry and Condensed Matter,
Dr. A. Paunescu Podeanu Street, No. 144, 300569 Timisoara, Romania.

EQUATIONS

$$E_{RHE} = E_{Ag/AgCl(sat. KCl)} + 0.059 \text{ pH} + E^{\circ}_{Ag/AgCl(sat. KCl)} \quad (\text{S-1})$$

$$\eta_{OER} = E_{RHE} - 1.23 \quad (\text{S-2})$$

$$\eta_{HER} = |E_{RHE}| \quad (\text{S-3})$$

$$\eta = b \times \log(j) + a \quad (\text{S-4})$$

$$j_{dl} = \frac{j_a + j_c}{2} \quad (\text{S-5})$$

$$EASA = \frac{C_{dl} \times S_{geom}}{C_s} \quad (\text{S-6})$$

where E_{RHE} / V is the converted potential vs. RHE; $E_{Ag/AgCl(sat. KCl)}$ / V is the measured potential vs. the Ag/AgCl(sat. KCl) reference electrode; $E^{\circ}_{Ag/AgCl(sat. KCl)} = 0.197$ V; η_{OER} / V is the O₂ evolution overpotential; η_{HER} / V is the H₂ evolution overpotential; η / V is the overpotential; j / A cm⁻² is the current density; b / V dec⁻¹ is the Tafel slope; j_{dl} / A cm⁻² is the capacitive current density; j_a / A cm⁻² is the absolute value of the anodic j corresponding to a given scan rate value, at an electrochemical potential value where there are only double-layer adsorption and desorption features; j_c / A cm⁻² is the absolute value of the cathodic j corresponding to a given scan rate value, at an electrochemical potential value where there are only double-layer adsorption and desorption features; $EASA$ / cm² is the electrochemically active surface area; C_{dl} / F cm⁻² is the electric double-layer capacitance; S_{geom} / cm² is the geometric surface of the electrode and C_s / F cm⁻² is the specific capacitance.¹⁻⁴

* Corresponding author. E-mail: b.taranu84@gmail.com; Phone: +40740955505
<https://doi.org/10.2298/JSC241004105T>

ELECTROCHEMISTRY DATA

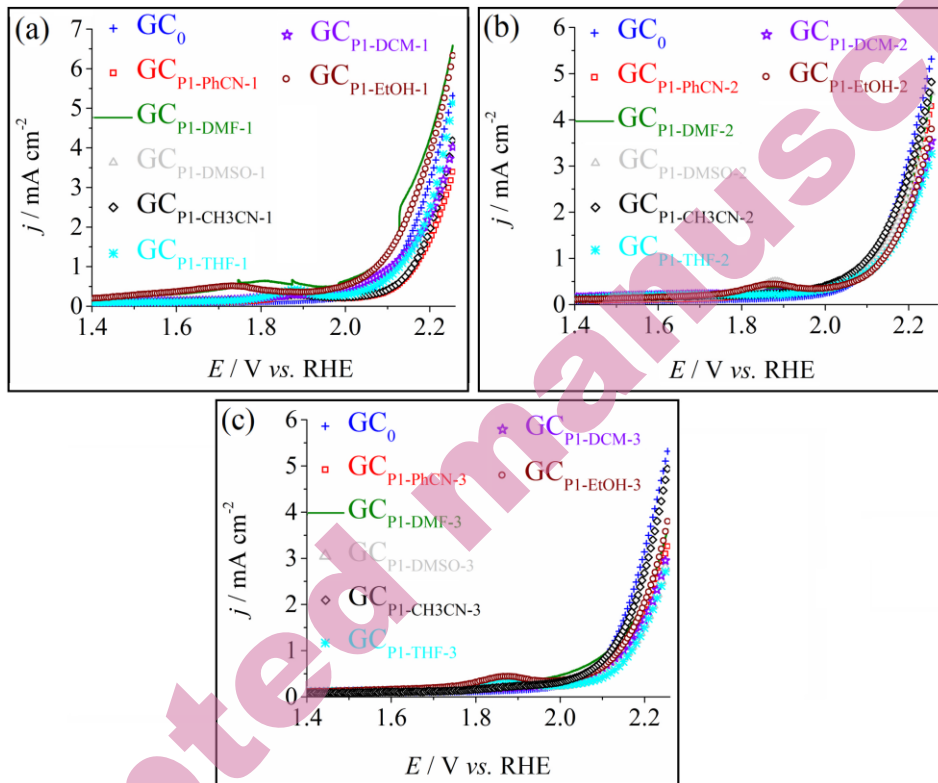


Fig. S-1. Anodic polarization curves recorded on GC_0 and on (a) $\text{GC}_{\text{PI-PhCN-1}}$, $\text{GC}_{\text{PI-DMF-1}}$, $\text{GC}_{\text{PI-DMSO-1}}$, $\text{GC}_{\text{PI-CH3CN-1}}$, $\text{GC}_{\text{PI-THF-1}}$, $\text{GC}_{\text{PI-DCM-1}}$ and $\text{GC}_{\text{PI-EtOH-1}}$; (b) $\text{GC}_{\text{PI-PhCN-2}}$, $\text{GC}_{\text{PI-DMF-2}}$, $\text{GC}_{\text{PI-DMSO-2}}$, $\text{GC}_{\text{PI-CH3CN-2}}$, $\text{GC}_{\text{PI-THF-2}}$, $\text{GC}_{\text{PI-DCM-2}}$ and $\text{GC}_{\text{PI-EtOH-2}}$ and (c) on $\text{GC}_{\text{PI-PhCN-3}}$, $\text{GC}_{\text{PI-DMF-3}}$, $\text{GC}_{\text{PI-DMSO-3}}$, $\text{GC}_{\text{PI-CH3CN-3}}$, $\text{GC}_{\text{PI-THF-3}}$, $\text{GC}_{\text{PI-DCM-3}}$ and $\text{GC}_{\text{PI-EtOH-3}}$. Electrolyte solution: 0.1 mol L⁻¹ H_2SO_4 . $v = 5 \text{ mV s}^{-1}$.

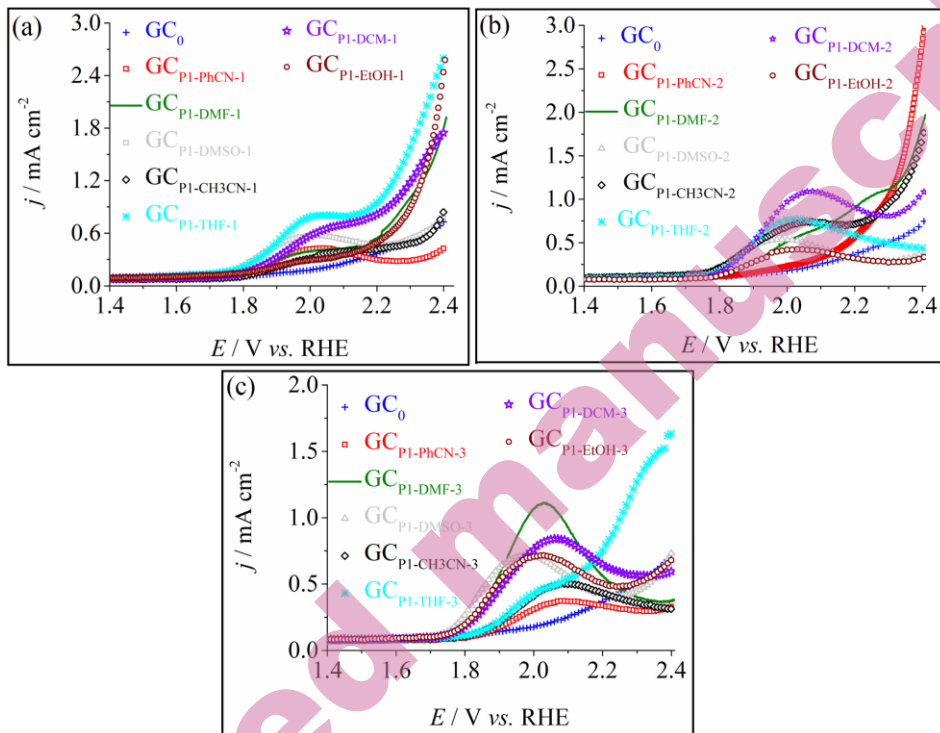


Fig. S-2. Anodic polarization curves recorded on GC_0 and on (a) $\text{GC}_{\text{P1}-\text{PhCN}-1}$, $\text{GC}_{\text{P1}-\text{DMF}-1}$, $\text{GC}_{\text{P1}-\text{DMSO}-1}$, $\text{GC}_{\text{P1}-\text{CH3CN}-1}$, $\text{GC}_{\text{P1}-\text{THF}-1}$, $\text{GC}_{\text{P1}-\text{DCM}-1}$ and $\text{GC}_{\text{P1}-\text{EtOH}-1}$; (b) $\text{GC}_{\text{P1}-\text{PhCN}-2}$, $\text{GC}_{\text{P1}-\text{DMF}-2}$, $\text{GC}_{\text{P1}-\text{DMSO}-2}$, $\text{GC}_{\text{P1}-\text{CH3CN}-2}$, $\text{GC}_{\text{P1}-\text{THF}-2}$, $\text{GC}_{\text{P1}-\text{DCM}-2}$ and $\text{GC}_{\text{P1}-\text{EtOH}-2}$ and (c) on $\text{GC}_{\text{P1}-\text{PhCN}-3}$, $\text{GC}_{\text{P1}-\text{DMF}-3}$, $\text{GC}_{\text{P1}-\text{DMSO}-3}$, $\text{GC}_{\text{P1}-\text{CH3CN}-3}$, $\text{GC}_{\text{P1}-\text{THF}-3}$, $\text{GC}_{\text{P1}-\text{DCM}-3}$ and $\text{GC}_{\text{P1}-\text{EtOH}-3}$. Electrolyte solution: 0.1 mol L⁻¹ KCl. $v = 5 \text{ mV s}^{-1}$.

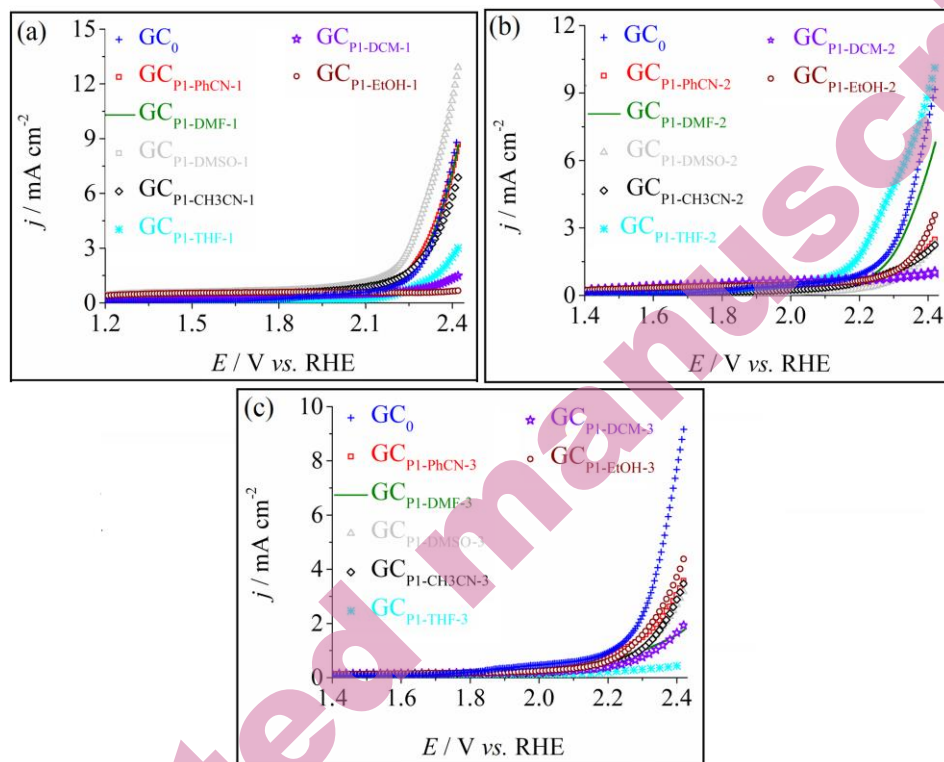


Fig. S-3. Anodic polarization curves recorded on GC_0 and on (a) $\text{GC}_{\text{PI-PhCN-1}}$, $\text{GC}_{\text{PI-DMF-1}}$, $\text{GC}_{\text{PI-DMSO-1}}$, $\text{GC}_{\text{PI-CH3CN-1}}$, $\text{GC}_{\text{PI-THF-1}}$, $\text{GC}_{\text{PI-DCM-1}}$ and $\text{GC}_{\text{PI-EtOH-1}}$; (b) $\text{GC}_{\text{PI-PhCN-2}}$, $\text{GC}_{\text{PI-DMF-2}}$, $\text{GC}_{\text{PI-DMSO-2}}$, $\text{GC}_{\text{PI-CH3CN-2}}$, $\text{GC}_{\text{PI-THF-2}}$, $\text{GC}_{\text{PI-DCM-2}}$ and $\text{GC}_{\text{PI-EtOH-2}}$ and (c) on $\text{GC}_{\text{PI-PhCN-3}}$, $\text{GC}_{\text{PI-DMF-3}}$, $\text{GC}_{\text{PI-DMSO-3}}$, $\text{GC}_{\text{PI-CH3CN-3}}$, $\text{GC}_{\text{PI-THF-3}}$, $\text{GC}_{\text{PI-DCM-3}}$ and $\text{GC}_{\text{PI-EtOH-3}}$. Electrolyte solution: 1 mol L^{-1} KOH. $v = 5 \text{ mV s}^{-1}$.

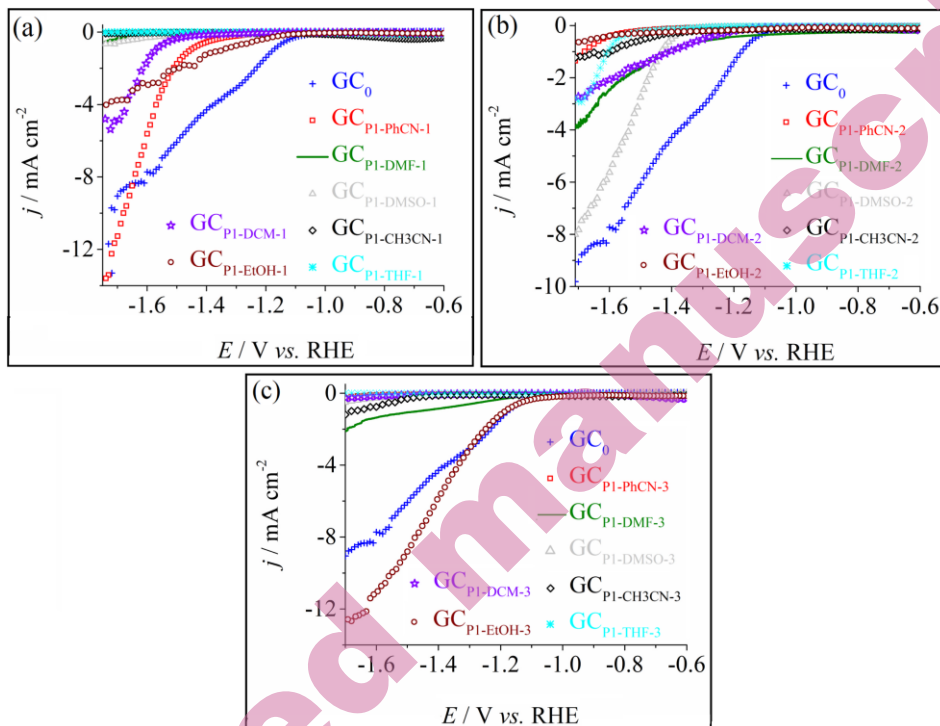


Fig. S-4. Cathodic polarization curves recorded on GC_0 and on (a) $\text{GC}_{\text{P}1\text{-PhCN-1}}$, $\text{GC}_{\text{P}1\text{-DMF-1}}$, $\text{GC}_{\text{P}1\text{-DMSO-1}}$, $\text{GC}_{\text{P}1\text{-CH3CN-1}}$, $\text{GC}_{\text{P}1\text{-THF-1}}$, $\text{GC}_{\text{P}1\text{-DCM-1}}$ and $\text{GC}_{\text{P}1\text{-EtOH-1}}$; (b) $\text{GC}_{\text{P}1\text{-PhCN-2}}$, $\text{GC}_{\text{P}1\text{-DMF-2}}$, $\text{GC}_{\text{P}1\text{-DMSO-2}}$, $\text{GC}_{\text{P}1\text{-CH3CN-2}}$, $\text{GC}_{\text{P}1\text{-THF-2}}$, $\text{GC}_{\text{P}1\text{-DCM-2}}$ and $\text{GC}_{\text{P}1\text{-EtOH-2}}$ and (c) on $\text{GC}_{\text{P}1\text{-PhCN-3}}$, $\text{GC}_{\text{P}1\text{-DMF-3}}$, $\text{GC}_{\text{P}1\text{-DMSO-3}}$, $\text{GC}_{\text{P}1\text{-CH3CN-3}}$, $\text{GC}_{\text{P}1\text{-THF-3}}$, $\text{GC}_{\text{P}1\text{-DCM-3}}$ and $\text{GC}_{\text{P}1\text{-EtOH-3}}$. Electrolyte solution: $0.1 \text{ mol L}^{-1} \text{ H}_2\text{SO}_4$. $v = 5 \text{ mV s}^{-1}$.

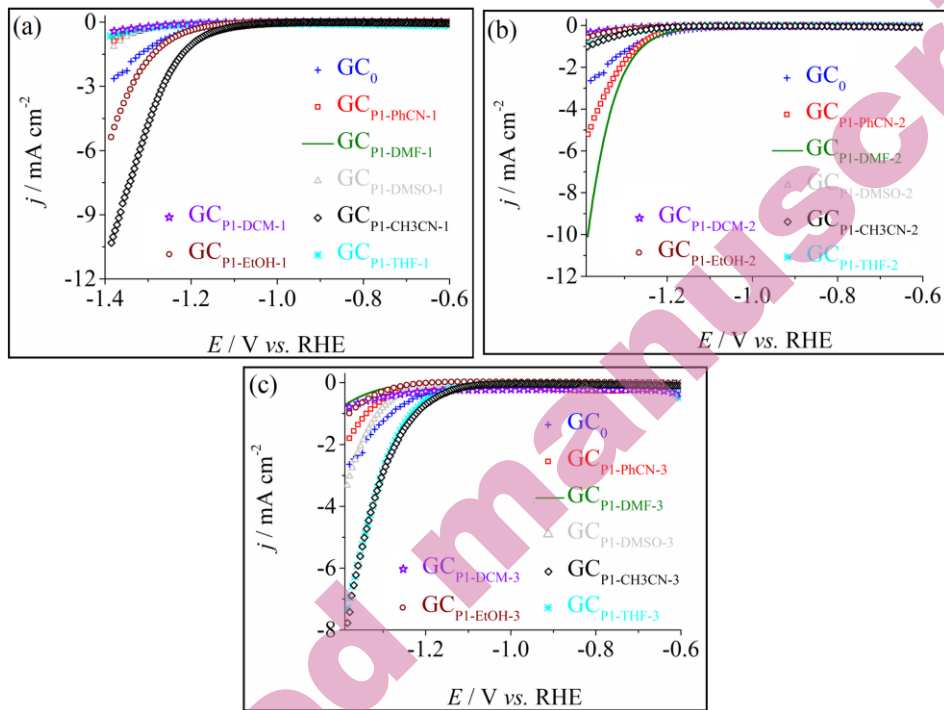


Fig. S-5. Cathodic polarization curves recorded on GC_0 and on (a) $\text{GC}_{\text{P}1-\text{PhCN}-1}$, $\text{GC}_{\text{P}1-\text{DMF}-1}$, $\text{GC}_{\text{P}1-\text{DMSO}-1}$, $\text{GC}_{\text{P}1-\text{CH}3\text{CN}-1}$, $\text{GC}_{\text{P}1-\text{THF}-1}$, $\text{GC}_{\text{P}1-\text{DCM}-1}$ and $\text{GC}_{\text{P}1-\text{EtOH}-1}$; (b) $\text{GC}_{\text{P}1-\text{PhCN}-2}$, $\text{GC}_{\text{P}1-\text{DMF}-2}$, $\text{GC}_{\text{P}1-\text{DMSO}-2}$, $\text{GC}_{\text{P}1-\text{CH}3\text{CN}-2}$, $\text{GC}_{\text{P}1-\text{THF}-2}$, $\text{GC}_{\text{P}1-\text{DCM}-2}$ and $\text{GC}_{\text{P}1-\text{EtOH}-2}$ and (c) on $\text{GC}_{\text{P}1-\text{PhCN}-3}$, $\text{GC}_{\text{P}1-\text{DMF}-3}$, $\text{GC}_{\text{P}1-\text{DMSO}-3}$, $\text{GC}_{\text{P}1-\text{CH}3\text{CN}-3}$, $\text{GC}_{\text{P}1-\text{THF}-3}$, $\text{GC}_{\text{P}1-\text{DCM}-3}$ and $\text{GC}_{\text{P}1-\text{EtOH}-3}$. Electrolyte solution: $0.1 \text{ mol L}^{-1} \text{ KCl}$. $v = 5 \text{ mV s}^{-1}$.

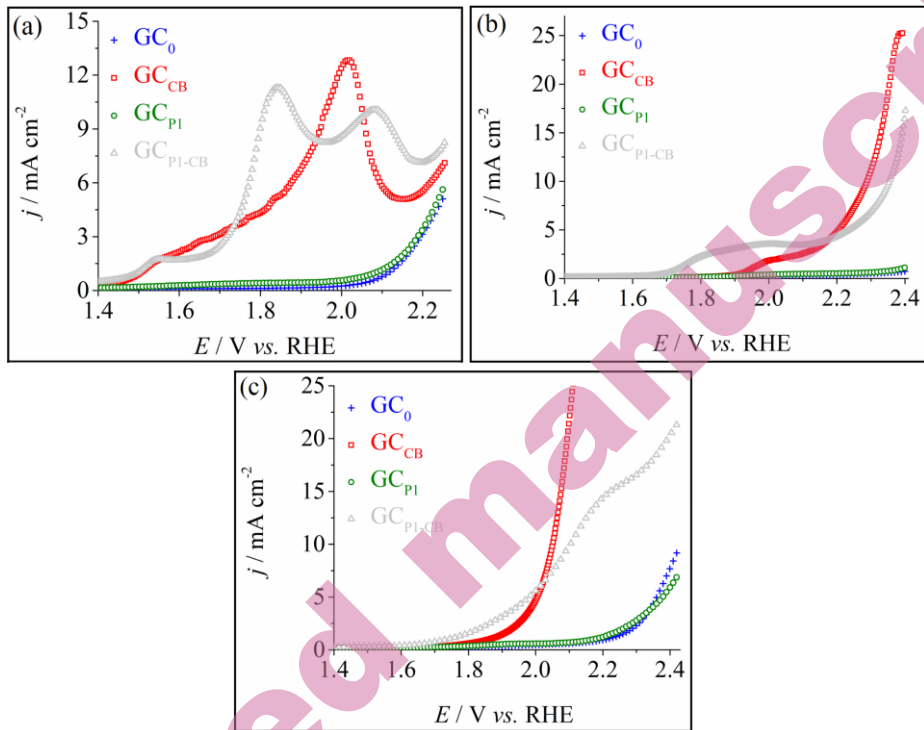


Fig. S-6. Anodic polarization curves recorded on GC₀, GC_{CB}, GC_{P1} and GC_{P1-CB} in the following electrolyte solutions: (a) 0.1 mol L⁻¹ H₂SO₄, (b) 0.1 mol L⁻¹ KCl and (c) 1 mol L⁻¹ KOH. $v = 5 \text{ mV s}^{-1}$.

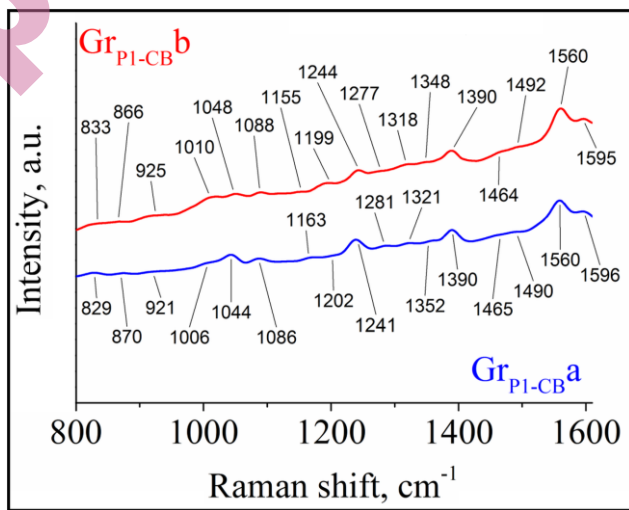


Fig. S-7. Raman spectra recorded on GC_{P1-CB} before an anodic stability experiment performed in 1 mol L⁻¹ KOH solution (GC_{P1-CB}^a) and after the experiment (GC_{P1-CB}^b).

TABLES

TABLE S-I. The HER activity of GC_{Pt-CB} and of other porphyrin-based electrodes

Catalyst @substrate	Environment	η_{HER} / mV at $j = -10 \text{ mA cm}^{-2}$	Tafel slope, mV dec ⁻¹	Ref.
Zn-TPP/G @Cu foil ^a	0.5 mol L ⁻¹ H ₂ SO ₄	~ 480 ^b	-	5
Zn-TAPP/G @Cu foil ^c	0.5 mol L ⁻¹ H ₂ SO ₄	~ 480 ^b	-	5
Zn-TPyP/G @Cu foil ^d	0.5 mol L ⁻¹ H ₂ SO ₄	~ 560 ^b	-	5
ZnTAPP-NA @GC ^e	1 mol L ⁻¹ KOH	546	121	6
CoTAPP-NA @GC ^f	1 mol L ⁻¹ KOH	470	110	6
CoTPP-SD @CFP ^g	1 mol L ⁻¹ KOH	475	-	7
CoCOP @CFP ^h	1 mol L ⁻¹ KOH	310	161	7
CoTCPP @FTO/Ag ⁱ	0.5 mol L ⁻¹ H ₂ SO ₄	666	264	8
CoTCPP polymer @FTO/Ag ^j	0.5 mol L ⁻¹ H ₂ SO ₄	475	197	8
CoTMPyP/ERGO @GC ^k	0.1 mol L ⁻¹ KOH	347 ^l	99	9
CoTMPyP/ERGO @GC	1 mol L ⁻¹ KOH	315 ^l	96	9
Co-2DP @Ti foil ^m	1 mol L ⁻¹ KOH	367 ^l	126	10
CoP-2ph-CMP-800 @GC ⁿ	1 mol L ⁻¹ KOH	360	121	11
CoP-3ph-CMP-800 @GC ^o	1 mol L ⁻¹ KOH	380	-	11
CoP-4ph-CMP-800 @GC ^p	1 mol L ⁻¹ KOH	440	-	11
G _{ZnP-DMF-1} ^q	1 mol L ⁻¹ KOH	520	150	2
Porphylar-based ink @carbon paper ^r	1 mol L ⁻¹ PBS	~ 770 ^s	227	12
G _{CB-PZn} ^t	0.1 mol L ⁻¹ KCl	1020	249	3
Fe-porphyrin polymer @carbon paper ^u	1 mol L ⁻¹ KOH	678	363	13
Co-porphyrin polymer @carbon paper ^v	1 mol L ⁻¹ KOH	437	195	13
Ni-porphyrin polymer @carbon paper ^w	1 mol L ⁻¹ KOH	644	345	13

Cu-porphyrin polymer @carbon paper ^x	1 mol L ⁻¹ KOH	436	236	13
Pt-TAPP/G @Cu foil ^y	0.5 mol L ⁻¹ H ₂ SO ₄	~ 550	-	5
2H-TAPP/G @Cu foil ^z	0.5 mol L ⁻¹ H ₂ SO ₄	600 ^{aa}	-	5
Ni-TAPP/G @Cu foil ^{ab}	0.5 mol L ⁻¹ H ₂ SO ₄	600 ^s	-	5
G _{P2-DMF} ^{ac}	0.5 mol L ⁻¹ H ₂ SO ₄	108	205	14
G _{P4-NiPh-THF} ^{ad}	1 mol L ⁻¹ KOH	430	140	15
[ERGO/CoTMPyP] ₇ / PDDA/4-ABA@GC ^{ae}	0.1 mol L ⁻¹ KOH	474 ^l	116	16
GC _{P1-CB}	1 mol L ⁻¹ KOH	770	135	This work

^a Zn-TPP = 5,10,15,20-tetraphenyl-21H,23H-porphine on single-layer graphene; ^b at -3 mA cm⁻²; ^c Zn-TAPP = 5,10,15,20-tetrakis(4-aminophenyl)-21H,23H-porphine on single-layer graphene; ^d Zn-TPyP = 5,10,15,20-tetrakis(4-pyridyl)-21H,23H-porphine on single-layer graphene; ^e ZnTAPP-NA = Zn(II) 5,10,15,20-tetra(4-aminophenyl)-21H,23H-porphyrin - ferrocene-1,1'-dicarbaldehyde; ^f CoTAPP-NA = Co(II) 5,10,15,20-tetra(4-aminophenyl)-21H,23H-porphyrin - ferrocene-1,1'-dicarbaldehyde; ^g CoTPP-SD@CFP = Co(II) 5,10,15,20-tetrakis(4-aminophenyl)porphyrin - salicylaldehyde@carbon fibre paper; ^h CoCOP = Co(II) 5,10,15,20-tetrakis(4-aminophenyl)porphyrin-based covalent organic polymer; ⁱ CoTCPP = Co(II) meso-tetra(4-carboxyphenyl)porphyrin; ^j CoTCPP polymer = crystalline Co(II) meso-tetra(4-carboxyphenyl)porphyrin-based polymeric system; ^k CoTMPyP/ERGO = tetrakis(N-methylpyridyl)porphyrinato cobalt / electrochemically reduced graphene oxide; ^l at -1 mA cm⁻²; ^m Co-2DP = multilayer 2D polymer based on Co(II) 5,10,15,20-tetrakis(4-aminophenyl)-21H,23H-porphyrin and 2,5-dihydroxyterephthalaldehyde; ⁿ CoP-2ph-CMP-800, ^o CoP-3ph-CMP-800 and ^p CoP-4ph-CMP-800 = conjugated mesoporous polymer based on Co-porphyrins and pyrolyzed at 800 °C; [ERGO/CoTMPyP]₇/PDDA/4-ABA@GC = multilayer films containing tetrakis(N-methylpyridyl)porphyrinato cobalt, on treated glassy carbon electrode; ^q G_{ZnP-DMF-1} = Zn(II) 5,10,15,20-tetrakis(4-pyridyl)-porphyrin drop-casted from DMF in one layer on graphite; ^r Porphvlar = organic polymer obtained from the condensation of terephthaloyl chloride and 5,10,15,20-tetrakis(4-aminophenyl)porphyrin; ^s at -7 mA cm⁻²; ^t G_{CB-PZn} = Zn(II) 5-(4-pyridyl)-10,15,20-tris(4-phenoxyphenyl)-porphyrin and Carbon Black drop-casted as catalyst ink on graphite; ^{u,v,w,x} Fe-porphyrin polymer, Co-porphyrin polymer, Ni-porphyrin polymer, Cu-porphyrin polymer = organic polymers obtained from the polymerization reaction of poly(*p*-phenylene terephthalamide) with 5,10,15,20-tetrakis(4-aminophenyl)porphyrin metallated with Fe, Co, Ni and Cu; ^y Pt-TAPP/G = Pt(II) 5,10,15,20-tetrakis(4-aminophenyl)-21H,23H-porphine on single-layer graphene; ^z 2H-TAPP/G = 5,10,15,20-tetrakis(4-aminophenyl)-21H,23H-porphine on single-layer graphene; ^{aa} at -9 mA cm⁻²; ^{ab} Ni-TAPP/G = Ni(II) 5,10,15,20-tetrakis(4-aminophenyl)-21H,23H-porphine on single-layer graphene; ^{ac} G_{P2-DMF} = Pt(II) 5-(3-hydroxyphenyl)-10,15,20-tris(3-methoxyphenyl)-porphyrin drop-casted on graphite substrate from N,N-dimethylformamide; ^{ad} G_{P4-NiPh-THF} = graphite substrate modified with suspension of nickel phosphite in solution of 5,10,15,20-tetrakis(4-methoxyphenyl)porphyrin dissolved in tetrahydrofuran; ^{ae} [ERGO@CoTMPyP]₇/PDDA/4-ABA@GC = multilayer films containing tetrakis(N-methylpyridyl)porphyrinato cobalt, on treated glassy carbon electrode.

REFERENCES

1. B.-O. Taranu, E. Fagadar-Cosma, *Processes* **10** (2022) 1 (<https://doi.org/10.3390/pr10030611>)
2. B.-O. Taranu, E. Fagadar-Cosma, *Nanomaterials-Basel* **12** (2022) 1 (<https://doi.org/10.3390/nano12213788>)
3. B.-O. Taranu, S. F. Rus, E. Fagadar-Cosma, *Coatings* **14** (2024) 1 (<https://doi.org/10.3390/coatings14081048>)
4. B. O. Taranu, S. D. Novaconi, M. Ivanovici, J. N. Goncalves, F. S. Rus, *Appl. Sci.-Basel* **12** (2022) 1 (<https://doi.org/10.3390/app12136821>)
5. S. Seo, K. Lee, M. Min, Y. Cho, M. Kim, H. Lee, *Nanoscale* **9** (2017) 3969 (<https://doi.org/10.1039/C6NR09428G>)
6. G. Cai, L. Zeng, L. He, S. Sun, Y. Tong, J. Zhang, *Chem.-Asian J.* **15** (2020) 1963 (<https://doi.org/10.1002/asia.202000083>)
7. A. Wang, L. Cheng, W. Zhao, X. Shen, W. Zhu, *J. Colloid Interf. Sci.* **579** (2020) 598 (<https://doi.org/10.1016/j.jcis.2020.06.109>)
8. Y. Wu, J. M. Veleta, D. Tang, A. D. Price, C. E. Botez, D. Villagran, *Dalton T.* **47** (2018) 8801 (<https://doi.org/10.1039/C8DT00302E>)
9. J. Ma, L. Liu, Q. Chen, M. Yang, D. Wang, Z. Tong, Z. Chen, *Appl. Surf. Sci.* **399** (2017) 535 (<https://doi.org/10.1016/j.apsusc.2016.12.070>)
10. H. Sahabudeen, H. Qi, B. A. Glatz, D. Tranca, R. Dong, Y. Hou, T. Zhang, C. Kuttner, T. Lehnert, G. Seifert, U. Kaiser, A. Fery, Z. Zheng, X. Feng, *Nat. Commun.* **7** (2016) 1 (<https://doi.org/10.1038/ncomms13461>)
11. H. Jia, Y. Yao, Y. Gao, D. Lu, P. Du, *Chem. Commun.* **52** (2016) 13483 (<https://doi.org/10.1039/C6CC06972J>)
12. Y. Ge, Z. Lyu, M. Marcos-Hernandez, D. Villagran, *Chem. Sci.* **13** (2022) 8597 (<https://doi.org/10.1039/D2SC01250B>)
13. N. Ocuane, Y. Ge, C. Sandoval-Pauker, D. Villagran, *Dalton T.* **53** (2024) 2306 (<https://doi.org/10.1039/D3DT03371F>)
14. I. Fratilesco, A. Lascu, B. O. Taranu, C. Epuran, M. Birdeanu, A.-M. Macsim, E. Tanasa, E. Vasile, E. Fagadar-Cosma, *Nanomaterials-Basel* **12** (2022) 1 (<https://doi.org/10.3390/nano12111930>)
15. B.-O. Taranu, E. Fagadar-Cosma, P. Sfirloaga, M. Poienar, *Energies* **16** (2023) 1 (<https://doi.org/10.3390/en16031212>)
16. D. Huang, J. Lu, S. Li, Y. Luo, C. Zhao, B. Hu, M. Wang, Y. Shen, *Langmuir* **30** (2014) 6990 (<https://doi.org/10.1021/la501052m>).